

WATER VAPOUR AS AN INERTING AGENT

BZ Dlugogorski*, RK Hichens, **EM Kennedy**

Department of Chemical Engineering

The University of Newcastle

Callaghan NSW 2308, AUSTRALIA

*Email: cgbzd@alinga.newcastle.edu.au

and

JW Bozzelli

Department of Chemical Engineering, Chemistry and Environmental Sciences

New Jersey Institute of Technology

Newark NJ 07102, USA

ABSTRACT

Water vapour can be used **as** a good essentially-inert agent **for** diluting mixtures of flammable gases since its inerting efficiency exceeds those of nitrogen and argon. **Its** disadvantages include the existence of the saturation concentration which may be insufficient for inerting (for gas temperatures below 80°C), and the inerting efficiency which is inferior to that of carbon dioxide. In this paper, we quantify the effect of water vapour on inerting natural gas-air mixtures in terms of flammability limits and laminar burning velocities. It is shown that, the adiabatic flame temperature at extinction of premixed natural gas-air-water vapour flames can be used to calculate the flammability limits at elevated temperatures of unburned gases, example equilibrium computations **are** performed at 100, 200 and 300°C. **A** C₁-C₂ chemical-kinetic mechanism is then verified against experimental data of the laminar burning velocities of dry natural gas-air flames and subsequently applied to predict the effect of humidity on flame propagation. We observe that water vapour displays a negligible chemical suppression and the physical suppression is mainly due to the effect of thermal capacity. The present results indicate that, for the effective inerting, the concentration of water vapour in the mixture of flammable gases needs to reach 36 and 44% for 100 and 300°C respectively. Furthermore, we discuss the relationship between the laminar burning velocities at extinction and the adiabatic temperature in the flammability limit to conclude that for these conditions to be equivalent the laminar burning velocity at extinction should be taken **as** approximately 15cm/s.

INTRODUCTION

With the compulsory phase-out of halons, and in some countries their mandatory destruction and ban on their use, the development of new fire suppressants has focused again on inert agents including gases (eg CO₂, or gas mixtures such **as** inergen and argonite; Dlugogorski et al, 1996), liquids (eg water mist; Mawhinney et al, 1994) and foams (eg compressed-air foams; Kim & Dlugogorski, 1997). *So* far, water vapour has not been seriously considered as a halon replacement although this gas is an efficient inerting agent, as is shown in the present paper.

Perhaps this lack of interest in water vapour can be explained by the fact that water vapour condenses under normal conditions and the agent must be delivered at elevated temperatures. However, in various industrial installations where steam is available because of the process requirements, fire-suppression and explosion-inerting systems may take an advantage of this opportunity. Stand-alone systems containing electrically-warmed superheated water which, upon activation, discharge fine-water mist mixed with water vapour can also be built with the existing technology. From this perspective, the objective of the present work is to evaluate the flammability properties of explosive

gas mixtures inerted by water vapour. This evaluation is conducted by calculating the flammability limits and laminar burning velocities of natural gas-air-water vapour mixtures at elevated temperatures.

The structure of the paper provides a framework for carrying out the evaluation. The next chapter describes the origin of the experimental data used to: (a) calculate the adiabatic flame temperature at extinction which then serves as a basis for obtaining the flammability diagram; and (b) validate the kinetic model for computations of the laminar burning velocities. This is followed by description of the computational methodology and by a separate chapter on results and discussion, which in turn is subdivided into four sections: (i) the results from flammability-limit calculations; (ii) the data from computation of the laminar burning velocities; (iii) the relationship between the laminar flame temperature and the laminar burning velocities at extinction; and (iv) the importance of physical and chemical factors affecting the extinguishment. The major findings of the present work are summarised in the conclusions.

EXPERIMENTAL DETAILS

The experimental data included in this paper have come from two sources. The limits of flammability of methane-air-inert mixture were taken from Coward & Jones (1952) and are replotted in Fig 1. Coward & Jones used the classical Bureau of Mines flammability apparatus in which the existence of upward propagating flames is observed in the open-ended glass tube 90cm in length and 5cm in diameter. The data for nitrogen and carbon dioxide were collected for premixed cold gases at 20°C. For determining the flammability limits with water vapour, the tube was heated to the temperature necessary to avoid condensation.

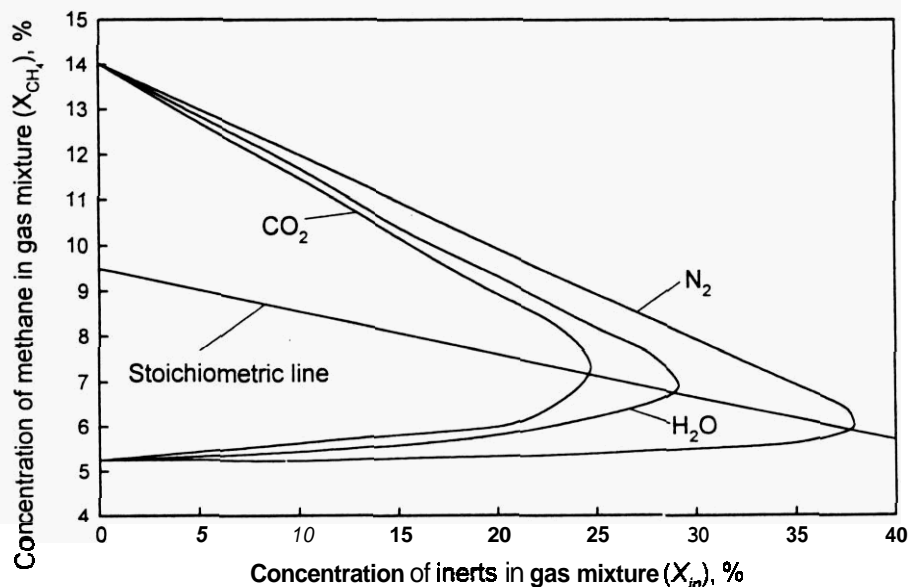


Figure 1. Limits of flammability of methane inerted with carbon dioxide, nitrogen and water vapour at atmospheric pressure; redrawn from Coward & Jones (1952).

The experimental data characterising the laminar-burning velocities of high ethane-content natural gas in desiccated mixtures with air at elevated temperatures were taken from Dlugogorski et al (1997). To obtain these data which are illustrated in Fig 2, we employed a conical Maché-Hebra nozzle burner and the total flame surface area determined from the schlieren photography. In volume percent, after removing minor species, the natural gas contained N₂ (1.23%), CH₄ (87.79%), CO₂ (1.88%) and C₂H₆ (9.04%). Because of its large ethane content, the present natural gas displayed slightly different

flammability properties than pure methane. These include reduced lower and upper flammability limits in air, increased concentration of inerts required in the limit of flammability, and slightly faster laminar burning velocities. Because of these considerations and the relevance of natural gas in process and petroleum industries we selected natural gas rather than methane as a fuel for this study.

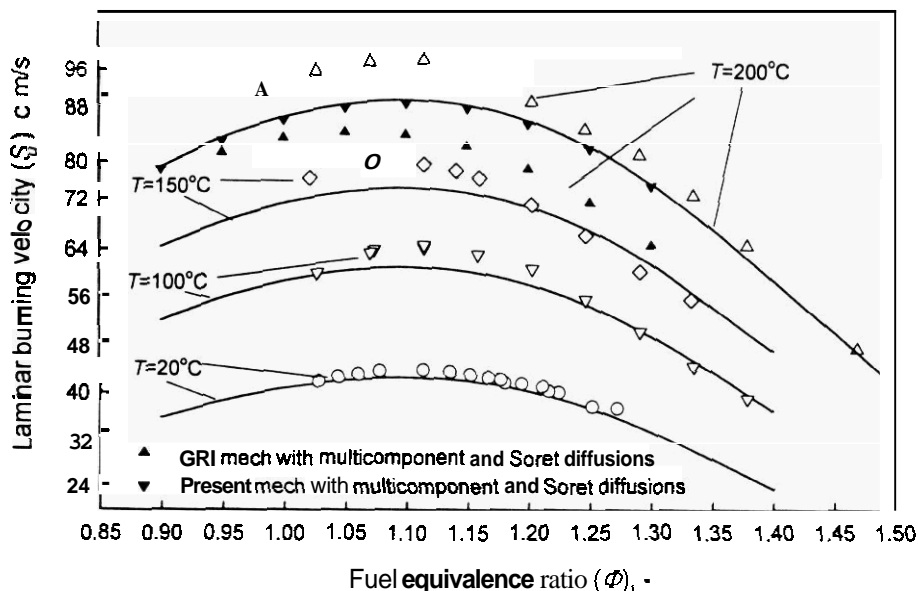


Figure 2. The comparison of experimental and modelling results for the combustion of desiccated natural gas in air. All open symbols signify the experimental data and the solid lines indicate the computational results using the present mechanism with no thermal and multicomponent diffusions. The filled triangles demonstrate the numerical data for which the multicomponent and Soret diffusions were included in the calculations. All calculations and experiments were performed at atmospheric pressure, and the temperature of the cold premixed inlet gases is indicated in the figure.

COMPUTATIONAL DETAILS

The equilibrium calculations were performed at constant pressure and enthalpy to obtain the adiabatic flame temperatures using the Chemkin interface (Chemkin kinetic libraries Ver 4.5; Kee et al 1989) to Stanjan III program (Ver 3.8C; Reynolds, 1988), in conjunction with the thermodynamic data base provided with the Gas Research Institute (GRI) 2.11 kinetic mechanism for natural-gas combustion (Bowman et al, 1997). The species included in the equilibrium calculations corresponded to those incorporated in the GRI 2.11 mechanism.

The laminar burning velocities were computed with Sandia's one-dimensional steady premixed laminar flame code (Premix Ver 2.55d; Kee et al, 1985) which operates on the layer of chemical-kinetic and multicomponent-transport (Ver 3.8; Kee et al, 1986) libraries. The code solves the conservation equations for mass, species and energy at constant pressure with no heat losses. Since, for the reacting system considered in the present paper, the calculated value of the laminar burning velocity is very sensitive to the number of grid points used in the calculations (Dlugogorski et al, 1997), all data points reported here were obtained from computations employing more than 1000 nodes. This was done initially by converging the program on a small domain and then by decreasing the GRAD and CURL parameters to 0.01. Because of the memory considerations we kept the maximum number of grid points allowed (NMAX) to 1250. Due to this finite (however large) size of the computational domain, a maximum 0.7% overestimation in the reported values of the laminar burning velocities (S_L) is expected.

The detailed C₁-C₂ mechanism for combustion of natural gas in air, as used in this paper, is included in the Appendix. The mechanism comprises 108 reactions and 26 species and is derived from the work of Bozzelli and his collaborators (Ho et al, 1992a&b; Ho & Bozzelli, 1992). The predictions from the mechanism are validated in Fig 2, where we compare the experimental results from the combustion of the desiccated natural gas with the modelling data, by varying the fuel equivalence ratio and the temperature of the cold gases entering the combustion zone. It is clear that, the model reproduces accurately the decreasing laminar burning velocities away from the fuel equivalence ratio of 1.1, but tends to underpredict the maximum S_v at the higher temperatures. The attempt to apply the GRI 2.11 mechanism (Bowman et al, 1997) led to even greater underprediction of the experimental data, as it is illustrated in Fig 2 for the case of 200°C.

In most of the calculations, the multicomponent and thermal diffusions were not turned on, by omitting the keywords TDIF and MULTI from the Premix input file. As illustrated in Fig 2, there is a marginal improvement in precision when multicomponent and Soret diffusions are accounted in the calculations (compare the solid line with the downward pointing triangles for 200°C) which does not justify the significant increase in the CPU cost for additional computations. Consequently, with the exception of part of Fig 2, all calculations reported here were carried out using the mixture-average transport coefficients in conjunction with the corrected diffusion velocity.

RESULTS and DISCUSSION

Flammability limits

It is generally accepted that combustion cannot be sustained when the adiabatic flame temperature drops below 1500K (Drysdale, 1985). From this perspective the concept of adiabatic flame temperature for the limit flames ($T_{ad,lim}$) serves as a convenient means to diagnose whether combustion takes place. Fundamentally, the situation is much more complex and the flame extinction arises due to the interplay among heat transfer, mass transfer, hydrodynamics and chemical kinetics. For simplicity, we have adopted $T_{ad,lim}$ for further considerations and have calculated the numerical values of $T_{ad,lim}$ along the flammability curves shown in Fig 1.

The results, presented in Fig 3, demonstrate that the calculated lower flammability limit occurs for the fuel equivalence ratio Φ of 0.53 and $T_{ad,lim}$ of 1533K. Subsequently, $T_{ad,lim}$ increases with Φ to reach a local maximum at around stoichiometric Φ , for all three inerting agents considered in Fig 1. In the limit of fuel rich flames, the extinction takes place at $T_{ad,lim}$ of 1864K for $\Phi=1.55$. This trend has been approximated by a least-squares low-degree polynomial, as illustrated in Fig 3:

$$T_{ad,lim} = 1450.3 + 92.7\Phi + 106.2\Phi^2. \quad 1$$

We then applied this polynomial fit to predict the flammability limits for inerting the preheated mixture of natural gas and air with water vapour, this is shown in Fig 4. Knowledge of flammability limits at high temperature is important for industrial risk assessment where flammable mixtures exist at elevated temperatures. In addition, a discharging water vapour-based fire or explosion suppression system would need to raise the temperature of the flammable-gas mixture diluted with water vapour to at least 80°C to avoid condensation below the inerting concentration.

Finally, we would like to comment on the expected cupburner extinction concentration for water vapour. It has been noted that the concentration of a suppressant needed for extinction of diffusion flames (such as those of cup burner) corresponds to the extinction concentration present for the limit premixed stoichiometric flames (Beyler, 1995). From this fact and from Fig 4, we estimate the cup-burner concentration to be around 38% for the mixture of air and water vapour delivered to the cup-burner apparatus at 100°C.

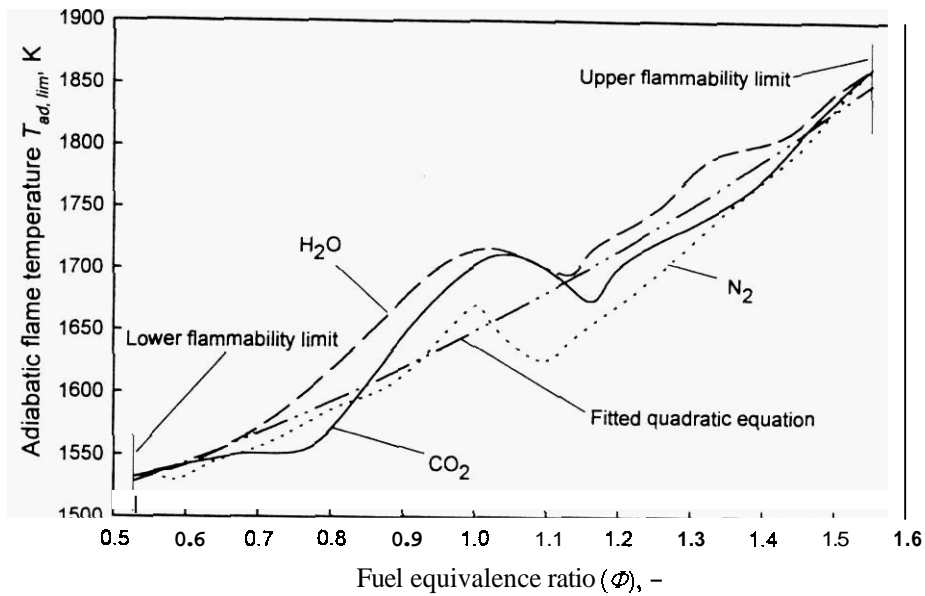


Figure 3. The relationship between the fuel equivalence ratio and the adiabatic flame temperature for the mitigated limit methane flames; the calculations are performed at atmospheric pressure (101.3 kPa), and 20°C for carbon dioxide and nitrogen, see the text describing Fig 1 for the explanation of water-vapour temperature.

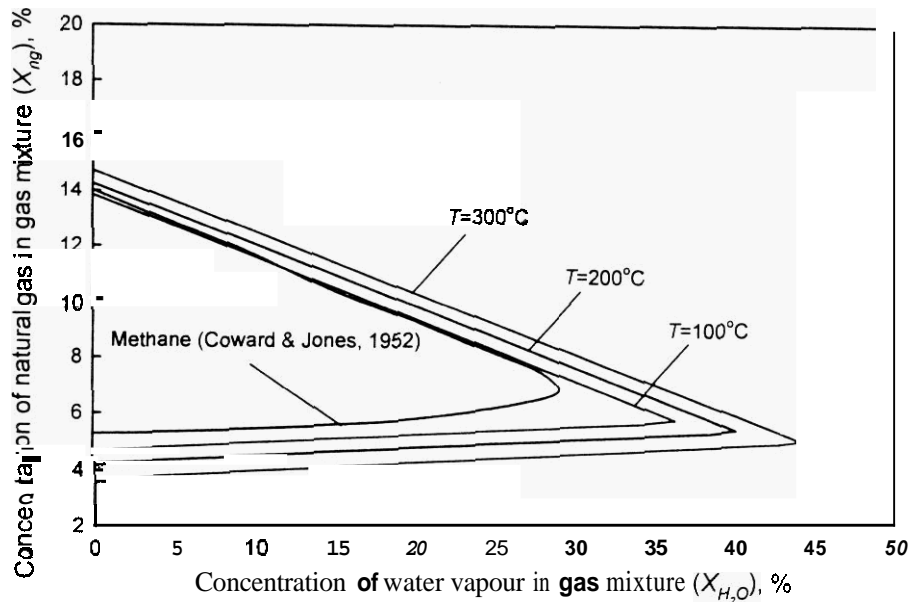


Figure 4. Calculated flammability diagram for 9.04% ethane-content natural gas at elevated temperatures and the atmospheric pressure.

Laminar burning velocities

Figures 5-7 summarise the computational results which illustrate the effect of addition of water vapour on mitigating the propagation of laminar natural gas-air flames. For example, Fig 5 illustrates that the maximum burning velocity does not shift from $\Phi=1.1$, except for $X_{H_2O}=30\%$, upon addition of

water vapour. Because of the lack of experimental data, we cannot conclude whether the flattening of S_u curve for $X_{H_2O}=20\%$ above $\phi=1.4$ is a reflection of physical behaviour or merely a computational artefact.

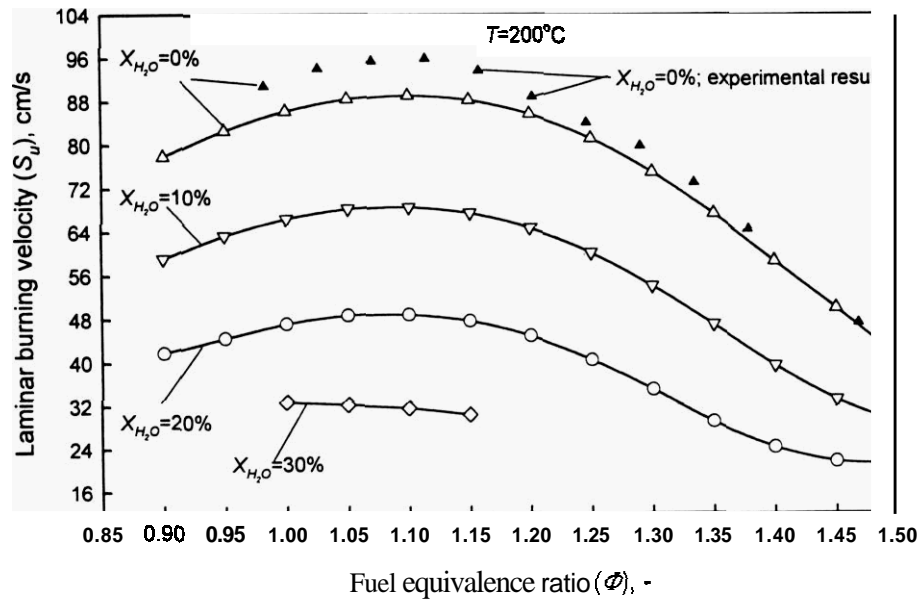


Figure 5. The reduction of the laminar burning velocity upon dilution of the premixed gases with water vapour at atmospheric pressure and 200°C.

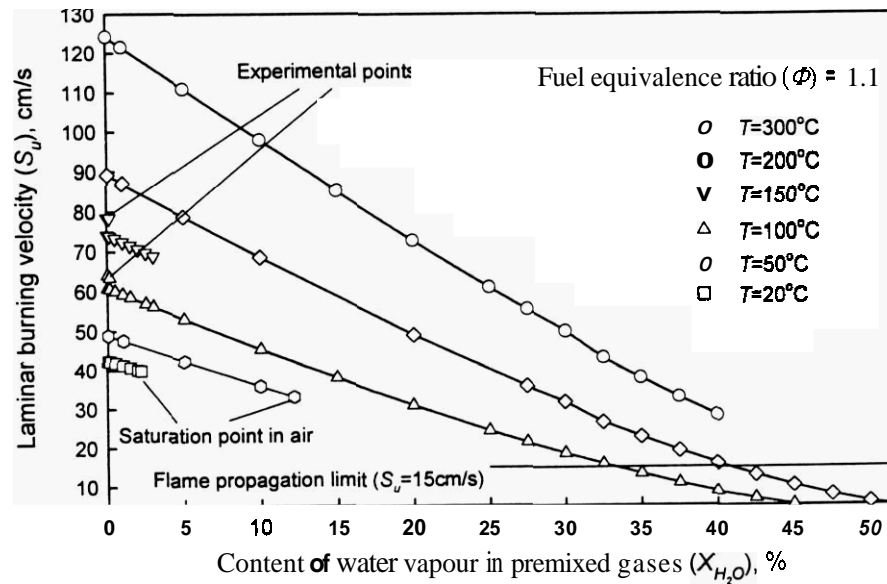


Figure 6. The laminar burning velocity of natural gas-air flames inerted with water vapour as function of temperature and water content, as calculated from the model.

Figure 6 demonstrates that water vapour seems to decrease the laminar burning velocity more significantly, with respect to the added amount of humidity, for gas mixtures at higher initial temperatures. In Fig 6, we introduced the flame propagation limit (to be explained in the next section) to demonstrate the approximate location of the limit of flammability of mitigated natural gas-air mixtures at elevated temperatures at the fuel equivalence ratio of 1.1. For example, at 100°C this limit

is around 32.5% of water vapour in the gas mixture. Figure 7 complements the information presented in Fig 6 and stresses that the addition of humidity moderates the upward trend of the laminar temperature with the increasing temperature of the premixed gases.

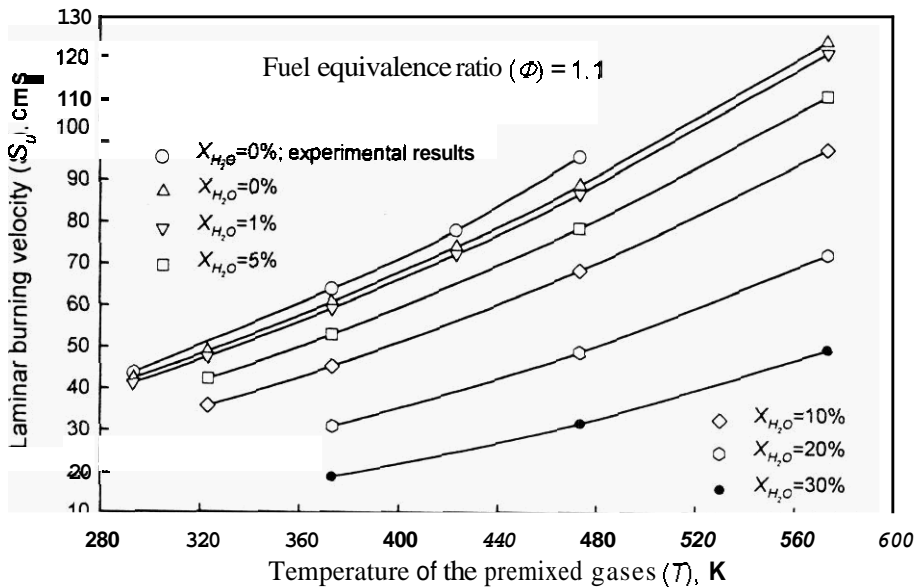


Figure 7. The effect of temperature on the propagation of laminar flames at different loadings of water vapour; computational results.

Adiabatic temperature and laminar burning velocity for the limit flames

The flammability limits presented at the beginning of this chapter depend on a number of fundamental physical and chemical processes occurring in flames, and also on the geometry of the experimental set-up. This is evident when one compares the flammability limits obtained from the Bureau of Mines apparatus (eg Zabetakis, 1965) with the more recent data from the tubular burner (Saito et al, 1995). In general, experimental systems that minimise flame stretch and reduce heat transfer rates away from the flame zone provide wider flammability limits. However, the theoretical boundaries on how wide these flammability limits can be do exist. These boundaries come from the calculation of the laminar burning velocities of adiabatic, planar, one-dimensional premixed flames. As S_u drops to zero, flames can no longer propagate and the theoretical limit is reached.

Unfortunately, the calculations of S_u close to the zero limit are not straightforward because of the difficulties in obtaining the convergence for a large number of grid point (more than 1000) which *is* needed for ensuring the computational precision. For example in Fig 6, we showed the calculated laminar burning velocities as low as 5cm/s for the mitigated natural-gas flames at 100 and 200°C (the limit at 0cm/s can be obtained by extrapolation), but we were not able to attain the convergence at 300°C for the water-vapour loading of more than 40%. Note that, the flammability diagram calculated in the zero limit of S_u depends on chemical-kinetic model used and provides too conservative estimates for practical applications.

To avoid these difficulties, we *argue* that for the flammability-limit calculations (via the computation of the laminar burning velocities) one should select a value of S_u which *is* consistent with the adiabatic flame temperature of the limit flames. This concept is illustrated in Fig 8. From Eq 1, we calculate $T_{ad,lim}$ for $\Phi=1.1$ as 1681K. This leads to $S_{u,lim}$ of 15cm/s for the cold gases at 100°C and slightly higher velocities at more elevated temperatures. From this consideration, we recommend that (conservatively) $S_{u,lim}$ of 15cm/s be used for calculating the extinction point corresponding to the

maximum burning velocity ($\phi=1.1$). Note that for the chemically active suppressants, $T_{ad,lim}$ will be higher due to the heat released in the recombination of H radicals, and so $S_{u,lim}$ of 15 cm/s would again provide a conservative estimate.

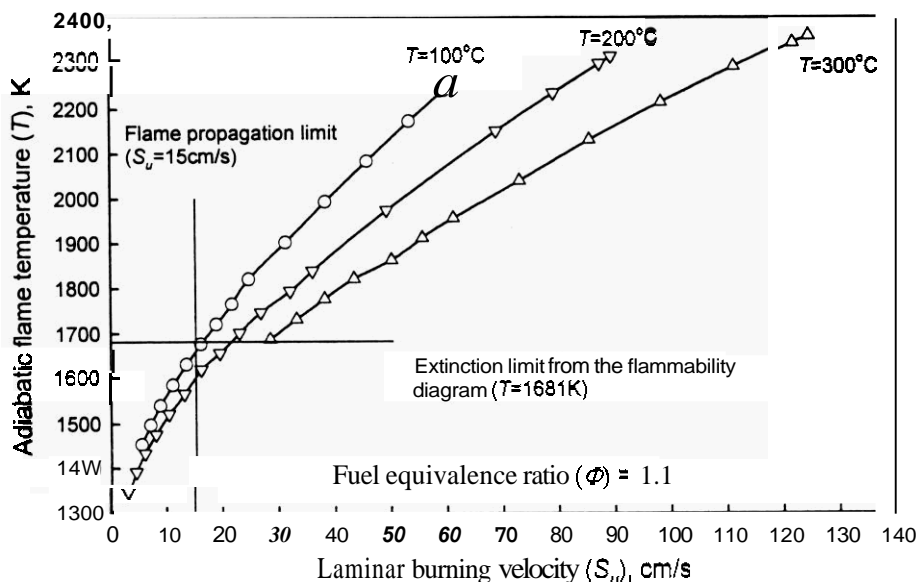


Figure 8. Equivalence of the adiabatic flame temperatures and the laminar burning velocities at the point of extinction.

Physical and chemical suppression

Babushok et al (1997) suggested a computational technique for evaluating the magnitude of various contributions toward the overall flame suppression of gaseous agents. In the first step, the chemical and physical suppression is separated by calculating the laminar burning velocities of fuel-air-suppressant mixtures with and without allowing the suppressant to participate in chemical reactions. In the second step, the contribution from physical suppression is redistributed between the effects of dilution and thermal capacity, by setting the suppressant's heat capacity to zero.

To carry out the calculations, we introduced an artificial water species which was not permitted to dissociate and to react chemically with other moieties present in the flames. In the second step, we kept the constants c_1 - c_3 for this species equal to zero in the thermodynamic data base (Kee et al, 1987). Figure 9 illustrates the results of these calculations. It is immediately obvious that water vapour displays negligible catalytic effect during flame mitigation and the suppression is mainly due to the effect of thermal capacity. The importance of the effect of thermal capacity increases with the addition of water vapour.

CONCLUSIONS

The present paper evaluated the effectiveness of water vapour as a gaseous agent for inerting flammable-gas mixtures. The results are also relevant to the design and operation of water vapour based fire-suppression systems. From the calculations and discussion presented in the paper, we draw the following conclusions:

- Water vapour in mixtures with flammable gases and vapours shows good fire and explosion mitigation properties. For example from the calculations, we estimate the cup burner value of

water vapour for 38%, and demonstrate that the laminar burning velocity of natural gas-air flames decreases rapidly with the addition of water vapour.

- There is a small but noticeable effect of temperature of cold premixed gases on the water-vapour inerting concentration; that is for 100 and 300°C, this concentration is 36 and 44%, respectively.
- The laminar burning velocity at flame extinction and the corresponding adiabatic temperature for limit flames can be taken as a starting point for practical calculations of flammability limits. It is proposed that $S_{u,lim}$ of 15cm/s and $T_{ad,lim}$ of 1681K are used to calculate the extinction of hydrocarbon flames with inerting agents at $\Phi=1.1$.
- At the fuel equivalence ratio of 1.1, water vapour shows a marginal effect of chemical suppression and the physical suppression is mostly due to thermal capacity. For all practical purposes, water vapour can be considered as an inert agent.

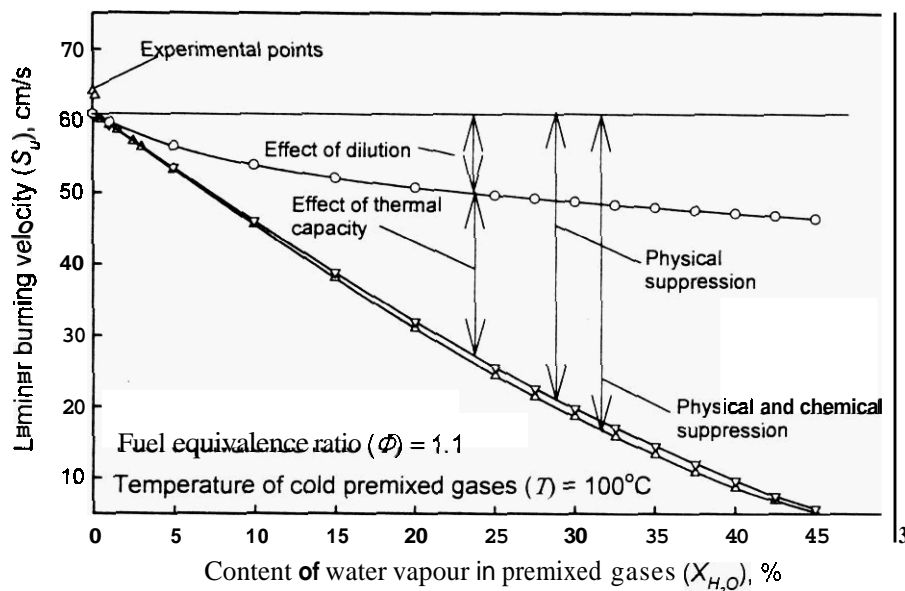


Figure 9. The importance of chemical and physical flame inhibition mechanisms displayed by water vapour.

ACKNOWLEDGMENTS

The authors wish to thank the Australian Research Council for providing financial support for the present work.

REFERENCES

- Babushok V, Noto T, Hamins A and Tsang W (1997) "Chemical and physical influences of halogenated fire suppressants", Halon *Options Technical Working Conf*, Albuquerque NM.
- Beyler C (1995) "Flammability Limits of Premixed and Diffusion Flames" in *The SFPE Handbook of Fire Protection Engineering*, NFPA, Quincy MA, 2:147-59.
- Bowman CT, Hanson RK, Davidson DF, Gardiner WC Jr, Lissianski V, Smith GP, Golden DM, Frenklach M and Goldenberg M (1997) "GRI-mech 2.11" http://www.me.berkeley.edu/gri_mech/.

- Coward HF and Jones GW (1952) *Limits of Flammability of Gases and Vapors*, Bull 503, US Bureau of Mines.
- Dlugogorski BZ, Kennedy EM and Moms KA (1996) "Thermal behaviour of cup burners", *Interflam '96, 7th Int Conf on Fire Scie & Tech*, 445-57.
- Dlugogorski BZ, Hichens RK, Kennedy EM and Bozzelli JW (1997) "Propagation of laminar flames in wet premixed natural gas-air mixtures", preprint, The University of Newcastle (submitted for publication).
- Drysdale D (1985) *An Introduction to Fire Dynamics*, Wiley, New York.
- Ho WP and Bozzelli JW (1992) "Validation of a mechanism for use in modelling CH_2Cl_2 and CH_3Cl combustion and/or pyrolysis" *24 Symp (In) on Comb*, 743-8.
- Ho WP, Barat RB and Bozzelli JW (1992a), "Thermal reactions of CH_2Cl_2 in H_2/O_2 mixtures: Implications for chlorine inhibition of CO conversion to CO_2 " *Comb & Flame* **88**, 265-95.
- Ho WP, Yu QR and Bozzelli JW (1992b) "Kinetic study on pyrolysis and oxidation of CH_3Cl in $\text{Ar}/\text{H}_2/\text{O}_2$ mixtures" *Comb Scie & Tech* **85(1/6)**, 23-63.
- Kee RJ, Grcar JF, Smooke MD and Miller JA (1985) *A Fortran Computer Program for Modeling Steady Laminar One-Dimensional Premixed Flames*, Sandia National Laboratories Report, SAND85-8240.
- Kee RJ, Dixon-Lewis G, Warnatz J, Coltrin ME and Miller JA (1986) *A Fortran Computer Code Package for the Evaluation of Gas-Phase Multicomponent Transport Properties*, Sandia National Laboratories Report, SAND86-8246.
- Kee RJ, Rupley FM and Miller JA (1987) *The Chemkin Thermodynamic Data Base*, Sandia National Laboratories Report, SAND87-8215B.
- Kee RJ, Rupley FM and Miller JA (1989) *Chemkin II: A Fortran Chemical Kinetics Package for the Analysis of Gas Phase Chemical Kinetics*, Sandia National Laboratories Report, SAND90-8009B.
- Kim AK and Dlugogorski BZ (1997) "Multipurpose overhead compressed-air foam system and its fire suppression performance", *J Fire Prot Eng* (in press).
- Mawhinney JR, Dlugogorski BZ and Kim AK (1994) "A closer look at the fire extinguishing properties of water mist", *4th Int Symp Fire Safety Scie*, 47-60.
- Reynolds WC (1988) "Stanjan: Ver 3.8C, May 1988" (as included with Chemkin II distribution), Stanford University.
- Saito N, Saso Y, Liao C and Ogawa Y (1995) "Flammability peak concentrations of halon replacements and their function as fire suppressants", in *Halon Replacements: Technology and Science*, Miziolek AW and Tsang W eds, ACS Symp Ser 611, ACS, Washington, 243-57.
- Zabetakis MG (1965) *Flammability Characteristics of Combustible Gases and Vapors*, Bull 627, US Bureau of Mines.

APPENDIX

Detailed C₁-C₂ mechanism for combustion of natural gas as used in the present study to model the propagation of one-dimensional steady premixed laminar flames; $k = A T^b e^{-E/RT}$. Some of the digits in the activation energies are not significant and are numerical artifacts due to the conversion from cal/mole to J/mole.

NO	Reaction	A, mole cm sec K	b	E, J/mole
1	C2H6=C2H5+H	6.22E+47	-9.8	465,470.0
2	C2H6+CH3=C2H5+CH4	2.70E-01	4.0	34,644.0
3	C2H6=CH3+CH3	5.34E+54	-11.1	469,487.0
4	C2H6+H=C2H5+H2	6.61E+13	0.0	15,062.0
5	C2H6+O=C2H5+OH	2.51E+13	0.0	26,778.0
6	C2H6+OH=C2H5+H2O	8.85E+09	1.0	7,573.0
7	C2H5=C2H4+H	1.83E+39	-7.8	220,999.0
8	C2H5+CH3=CH4+C2H4	5.50E+11	0.0	0.0
9	C2H5+H=CH3+CH3	1.35E+22	-2.2	29,288.0
10	C2H5+O=CH2O+CH3	1.00E+13	0.0	0.0
11	C2H5+O2=C2H4+HO2	2.00E+12	0.0	20,887.0
12	C2H5+HO2=C2H4+H2O2	3.01E+11	0.0	0.0
13	C2H5+CH3O=C2H6+CH2O	2.41E+13	0.0	0.0
14	C2H5+CH2O=CHO+C2H6	5.50E+03	2.8	24,518.0
15	C2H4=C2H3+H	8.53E+30	-5.9	494,716.0
16	C2H4=C2H2+H2	8.52E+43	-8.3	507,268.0
17	C2H4+OH=C2H3+H2O	1.58E+04	2.8	17,460.0
18	C2H4+CH3=CH4+C2H3	4.20E+11	0.0	46,497.0
19	C2H4+O2=C2H3+HO2	4.22E+13	0.0	241,095.0
20	C2H4+H=C2H3+H2	6.92E+14	0.0	60,668.0
21	C2H3=C2H2+H	6.24E+29	-5.3	194,556.0
22	C2H3+O2=C2H2+HO2	1.21E+11	0.0	0.0
23	C2H3+O2=CHO+CH2O	3.97E+12	0.0	-1046.0
24	C2H2+O2=C2H+HO2	1.21E+13	0.0	311,792.0
25	C2H2+O=CO+CH2	4.10E+08	1.5	7,113.0
26	C2H2+O=HCCO+H	1.02E+07	2.0	7,950.0
27	C2H2+OH=C2H+H2O	1.45E+04	2.7	50,375.0
28	C2H2+OH=CH2CO+H	3.20E+11	0.0	837.0
29	C2H+O2=CO+CHO	2.41E+12	0.0	0.0
30	C2H+H2=C2H2+H	1.15E+13	0.0	12,050.0
31	C2H+CH4=C2H2+CH3	1.81E+12	0.0	2,092.0
32	C2H+OH=CH2+CO	1.81E+13	0.0	0.0
33	C2H+OH=C2H2+O	1.81E+13	0.0	0.0
34	HCCO+H=CH2s+CO	3.00E+13	0.0	0.0
35	CH2CO+O=CH2+CO2	1.74E+12	0.0	5648.0
36	CH2CO+H=HCCO+H2	5.00E+13	0.0	33,472.0
37	CH2CO+O=HCCO+OH	1.00E+13	0.0	33,472.0
38	CH2CO+OH=HCCO+H2O	7.50E+12	0.0	8,368.0
39	CH2CO+M=CH2+CO+M	3.00E+15	0.0	317,900.0
40	CH2CO+OH=CHO+CH2O	2.80E+13	0.0	0.0
41	CH2CO+H=CH3CO	1.50E+04	2.8	2815.0
42	CH2s+M=CH2+M	1.00E+13	0.0	0.0
43	CH2s+O2=CO+H2O	2.41E+11	0.0	0.0
44	CH2s+CH4=C2H5+H	9.43E+12	-0.1	27,698.0
45	CH2s+CH4=CH3+CH3	3.45E+22	-2.5	31,213.0
46	CH2s+CH4=C2H6	5.78E+46	-10.3	53,681.0
47	CH2s+H2=CH4	3.82E+25	-4.5	15,774.0
48	CH2s+H2=CH3+H	1.27E+14	-0.1	544.0
49	CH4=CH3+H	1.03E+33	-5.6	467,813.0
50	CH4+H=CH3+H2	1.55E+14	0.0	46,024.0

51	CH4+O2=CH3+HO2	4.04E+13	0.0	238,111.0
52	CH4+O=CH3+OH	1.02E+09	1.5	35,982.0
53	CH4+OH=CH3+H2O	1.93E+05	2.4	8,828.0
54	CH4+HO2=CH3+H2O2	2.00E+13	0.0	75,312.0
55	CH3+O2=CH2O+OH	3.59E+09	-0.1	42,468.0
56	CH3+O2=CH3O+O	2.88E+15	-1.1	129,076.0
57	CH3+O=CH2O+H	7.00E+13	0.0	0.0
58	CH3+OH=CH3O+H	3.87E+12	-0.2	57,492.0
59	CH3+HO2=CH3O+OH	2.00E+13	0.0	0.0
60	CH3+CH2O=CH4+CHO	1.00E+11	0.0	25,481.0
61	CH3O+O2=CH2O+HO2	6.62E+10	0.0	10,878.0
62	CH3O+M=CH2O+H+M	1.00E+14	0.0	105,018.0
63	CH3O+CO=CO2+CH3	1.57E+13	0.0	49,371.0
64	CH3O+HO2=CH2O+H2O2	3.01E+11	0.0	0.0
65	CH3O+CH3=CH4+CH2O	2.41E+13	0.0	0.0
66	CH3O+O=OH+CH2O	6.03E+12	0.0	0.0
67	CH3O+OH=H2O+CH2O	1.81E+13	0.0	0.0
68	CH3O+H=CH2O+H2	1.99E+13	0.0	0.0
69	CH3O+CH2=CH3+CH2O	1.81E+13	0.0	0.0
70	CH2O+H=CHO+H2	2.50E+13	0.0	16,694.0
71	CH2O+O=CHO+OH	3.50E+13	0.0	14,686.0
72	CH2O+OH=CHO+H2O	3.00E+13	0.0	4,979.0
73	CH2O+HO2=CHO+H2O2	1.00E+12	0.0	33,472.0
74	CH2O+M=CHO+H+M	5.00E+16	0.0	318,821.0
75	CH2O+O2=CHO+HO2	2.05E+13	0.0	162,946.0
76	CH2+CH4=CH3+CH3	1.82E+05	0.0	0.0
77	CH2+H2=CH3+H	3.01E+09	0.0	0.0
78	CH2+H2O=CH3+OH	9.64E+07	0.0	0.0
79	CH2+O2=CH2O+O	1.00E+14	0.0	15,481.0
80	CHO+M=H+CO+M	2.50E+14	0.0	70,249.0
81	CHO+H=CO+H2	2.00E+14	0.0	0.0
82	CHO+O2=CO+HO2	5.12E+13	0.0	7071.0
83	CHO+O=CO+OH	3.01E+13	0.0	0.0
84	CHO+O=H+CO2	3.01E+13	0.0	0.0
85	CHO+OH=CO+H2O	3.01E+13	0.0	0.0
86	CO+OH=CO2+H	4.40E+06	1.5	-3100.0
87	CO+HO2=CO2+OH	5.80E+13	0.0	95,956.0
88	CO+O2=CO2+O	2.50E+12	0.0	199,995.0
89	CO+O+M=CO2+M	6.17E+14	0.0	12,552.0
90	H+O2=O+OH	1.69E+17	-0.9	72,760.0
91	H+O2+M=HO2+M	1.42E+18	-0.8	0.0
92	H+H2O=H2+OH	4.60E+08	1.6	77,655.0
93	H+OH+M=H2O+M	7.50E+23	-2.6	0.0
94	H+O+M=OH+M	2.29E+14	0.0	16,318.0
95	H+HO2=OH+OH	1.69E+14	0.0	3,640.0
96	H+HO2=H2+O2	6.62E+13	0.0	8,912.0
97	H+H2O2=H2+HO2	4.82E+13	0.0	33263.0
98	H+H2O2=OH+H2O	2.41E+13	0.0	16,610.0
99	H2+M=H+H+M	4.57E+19	-1.4	436,768.0
100	H2+O=H+OH	1.08E+04	2.8	24,769.0
101	O+H2O=OH+OH	1.50E+10	1.1	72,132.0
102	O+H2O2=HO2+OH	9.63E+06	2.0	16,610.0
103	O+HO2=OH+O2	2.00E+13	0.0	0.0
104	OH+HO2=H2O+O2	2.00E+13	0.0	0.0
105	OH+H2O2=HO2+H2O	1.75E+12	0.0	1339.0
106	O2+M=O+O+M	1.20E+14	0.0	449,998.0
107	O2+H2O2=HO2+HO2	5.42E+13	0.0	166,272.0
108	H2O2+M=OH+OH+M	1.29E+33	4.9	222,798.0